JACS
JOURNAL OF THE AMERICAN CHEMICAL SOCIETY

Article

pubs.acs.org/JACS

Qualitative Analysis of Bulk-Heterojunction Solar Cells without Device Fabrication: An Elegant and Contactless Method

Derya Baran,*[,†] Ning Li,[†] Anne-Catherine Breton,[§,∥] Andres Osvet,[†] Tayebeh Ameri,[†] Mario Leclerc,[§] and Christoph J. Brabec*[,†,‡]

[†]Institute of Materials for Electronics and Energy Technology (i-MEET), Friedrich-Alexander-University of Erlangen-Nürnberg, Martensstrasse 7, 91058, Erlangen, GERMANY

[‡]Bavarian Center for Applied Energy Research (ZAE Bayern), Haberstr. 2a, 91058 Erlangen, GERMANY

[§]Université Laval, Department of Chemistry, Pavillon Alexandre-Vachon, Bureau 2240-C1045, Avenue de la Medicine, G1 V 0A6 Québec, QC, Canada

Supporting Information

ABSTRACT: The enormous synthetic efforts on novel solar cell materials require a reliable and fast technique for the rapid screening of novel donor/acceptor combinations in order to quickly and reliably estimate their optimized parameters. Here, we report the applicability of such a versatile and fast evaluation technique for bulk heterojunction (BHJ) organic photovoltaics (OPV) by utilizing a steady-state photoluminescence (PL) method confirmed by electroluminescence (EL) measurements. A strong relation has been observed between the residual singlet emission and the charge transfer state emission in the blend. Using this relation, a figure of merit (FOM) is defined from photoluminescence and also electroluminescence measurements for qualitative analysis and shown to precisely anticipate the optimized blend parameters of bulk heterojunction films. Photoluminescence allows contactless evaluation of the photoactive layer and can be used to predict the optimized conditions for the best polymer−fullerene combination. Most interestingly, the contactless, PL-based FOM method has the potential to be integrated as a fast and reliable inline tool for quality control and material optimization.

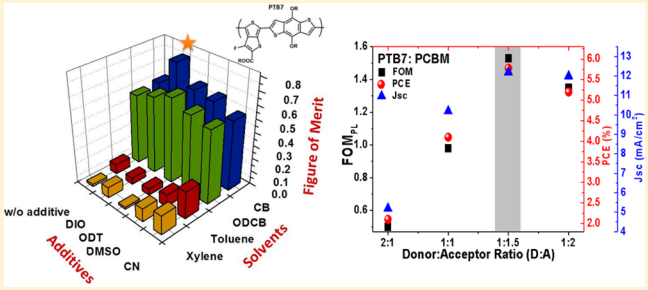

INTRODUCTION

Power conversion efficiencies (PCE) of organic photovoltaics (OPV) have already exceeded the 10% milestone.[1] This significant increase has been achieved by introducing innovative materials and device structures.[2,3] However, very few reliable techniques for the rapid screening of semiconducting materials as well as processing technologies were developed for the OPV area.[4−7] Controlling the morphology in the photoactive layer is one of the key issues to optimize the exciton harvesting, charge transfer, and charge transport processes at the donor/acceptor (D/A) interface. There are many methods, such as optimization of the D/A ratio,[8] use of different solvent mixtures,[9,10] additives,[11,12] thermal annealing,[13] among others, to control the microstructure of the photoactive layer and to improve the device performance. Yet, design and the optimization of high-performance materials is still a significant challenge for mass production of high-efficiency OPV devices. When a new polymer is introduced to the OPV field, it should be fully screened to find optimized parameters. Frequently, this is carried out with a herculean workload of complete device fabrication and characterization runs, taking a lot of time and effort. There are several techniques that can provide information on the quality of a solar cell in terms of its electrical and device properties such as charge extraction, transient photovoltage, impedance spectroscopy, and electroluminescence.[14−17] All these techniques require the completion of a full OPV device. On the other hand, there are very few rapid screening techniques which do not require electrical contacts suitable to gain insight in the PCE potential of the composites.

Photoluminescence (PL) is known as a fast, easy, and powerful spectroscopic tool which provides injection level dependent information about radiative recombination.[18] In addition, the method is contactless and is sensitive to both radiative singlet state transitions as well as low energy recombination transitions at the D/A interface. Photoluminescence from such interfacial charge transfer (CT) states (PL_{CT}) has been shown to be a sensitive probe for geminate recombination.[19−23] In addition to steady-state photoluminescence, related optical methods such as delayed photoluminescence or electroluminescence can be used to gain information related to free carrier, or nongeminate recombina-

Received: April 1, 2014
Published: July 8, 2014

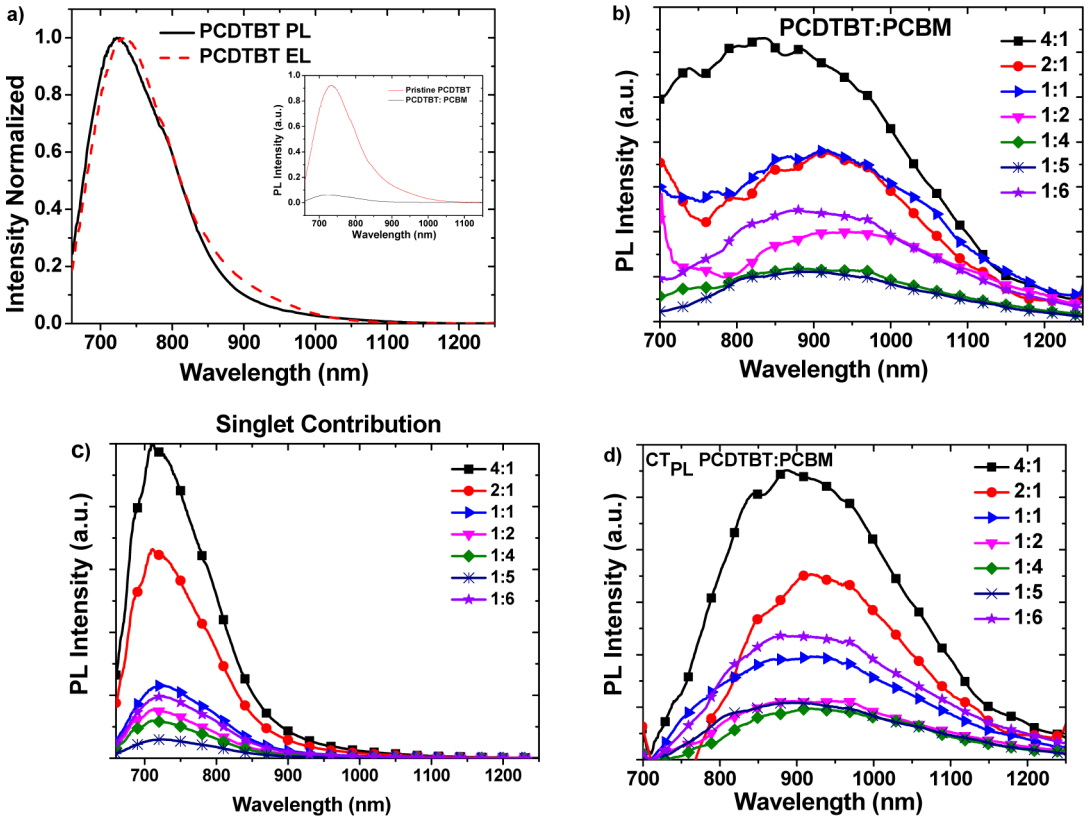

Figure 1. (a) Normalized PL and EL spectra of pristine PCDTBT and PL quenching of PCDTBT/$PC_{60}BM$ (inset), (b) PL spectra of PCDTBT/$PC_{60}BM$ blends, (c) composite residual PCDTBT singlet emission contribution in the blend, and (d) subtracted photoluminescence spectra of PCDTBT/$PC_{60}BM$ heterojunction with different stoichiometries. The relative PL emissions are corrected for the optical density of materials.

tion, including the effects of transport and electrical resistance in the bulk.[24,25]

In order to maximize the PCE of a material with a given band gap E_g, it is essential to convert as high number of absorbed photons as possible into collected charge carriers. This property strongly depends on the tightly bounded electron–hole pair (exciton) properties which limit the organic solar cell efficiencies.[26] Due to the low dielectric constant of the organic absorbers, a type II heterojunction is required for efficient charge separation. After exciton separation, charge carriers form a Coulombically bounded charge transfer (CT) state with energy E_{CT}. This energy can be determined from spectroscopic methods and theoretical calculations.[27−30] There have been many studies correlating the CT state energy, offset, or intensity to the open-circuit voltage (V_{OC}), energy losses, and the photocurrent generation yield in organic solar cells. However, to our knowledge, the residual singlet emission from a polymer has not been considered in these correlations so far. It is either ignored because the intensity is often relatively low or subtracted from the blend spectra to obtain the pristine CT signals.[31]

In this work, we present an interesting relation between the ratio of the CT emission and singlet emission intensity and the photovoltaic performance of polymer–fullerene composites. We define a figure of merit (FOM) and demonstrate that this FOM can be used as an indication for determining the optimized processing parameters in a polymer–fullerene system without full device fabrication. In particular, we show that the photocurrent generation yield in the blends leading to the optimized performance can be estimated qualitatively with this FOM using simple thin active layer films.

Two independent but essential steps along the photoinduced charge generation are photoinduced charge transfer, forming a CT state and preventing singlet emission. Therefore, the presence of residual singlet emission in the blend is indicative of a loss mechanism. Instead, the observation of CT state emission is taken as an indication that an electronic state with a higher probability of photocurrent generation is formed. We define a FOM by simply dividing the relative intensity of CT emission (I_{CT}) by the relative intensity of singlet emission (I_{SI-S0}) and expect that a higher FOM will indicate less singlets and more CT states formed and will thus yield a higher charge generation in the blend.

$$\text{figure of merit} = \frac{I_{CT}}{I_{SI-S0}} \tag{1}$$

It is noteworthy to mention also considering solely I_{CT} or I_{SI-S0} as an indicator for photocurrent generation is not enough, because absolute photoluminescence quenching should be considered. The method is also confirmed using the same eq 1 from electroluminescence measurements where CT energy can be defined easily and the contact and transport phenomena are included.

Several polymer systems including commercial poly(3-hexyl thiophene) (**P3HT**), a copolymer from 4,4′-bis(alkyl)dithieno-[3,2-b:2′,3′-d]silole) (Si-CPDT) and 5-bis(thiophen-2-yl)-thiazole[5,4-*d*]thiazole (TzTz) (**KP115**), a newly synthesized polymer poly-[*N*-9′-heptadecanyl-2,7-cabazole-*alt*-5,5-(5′,8′-di-2-thinenyl-(2′,3′-bis(5″-octylthiophene-2″-yl)quinoxaline))]-(**PCDTQxTh-C8**), a polycarbazole derivative poly[[9-(1-octylnonyl)-9H-carbazole-2,7-diyl]-2,5-thiophenediyl-2,1,3-

dx.doi.org/10.1021/ja503134j | J. Am. Chem. Soc. 2014, 136, 10949−10955

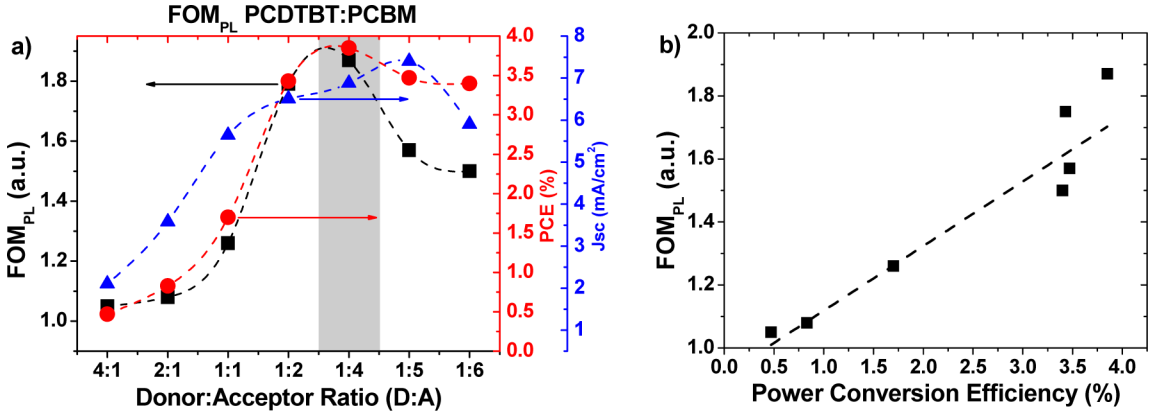

Figure 2. (a) FOM_{PL}, PCE, and J_{SC} trends as a function of PCDTBT/$PC_{60}BM$ ratio, (b) the relation between FOM_{PL} and the PCDTBT/$PC_{60}BM$ device efficiencies. The dashed lines are guides to the eye; the symbols are the measurement points. PL and *J*–*V* characteristics of the blends were measured from the same active layer. The devices are measured under the illumination of a lamp resembling the AM 1.5 standard spectrum with an intensity of 100 mW/cm^2.

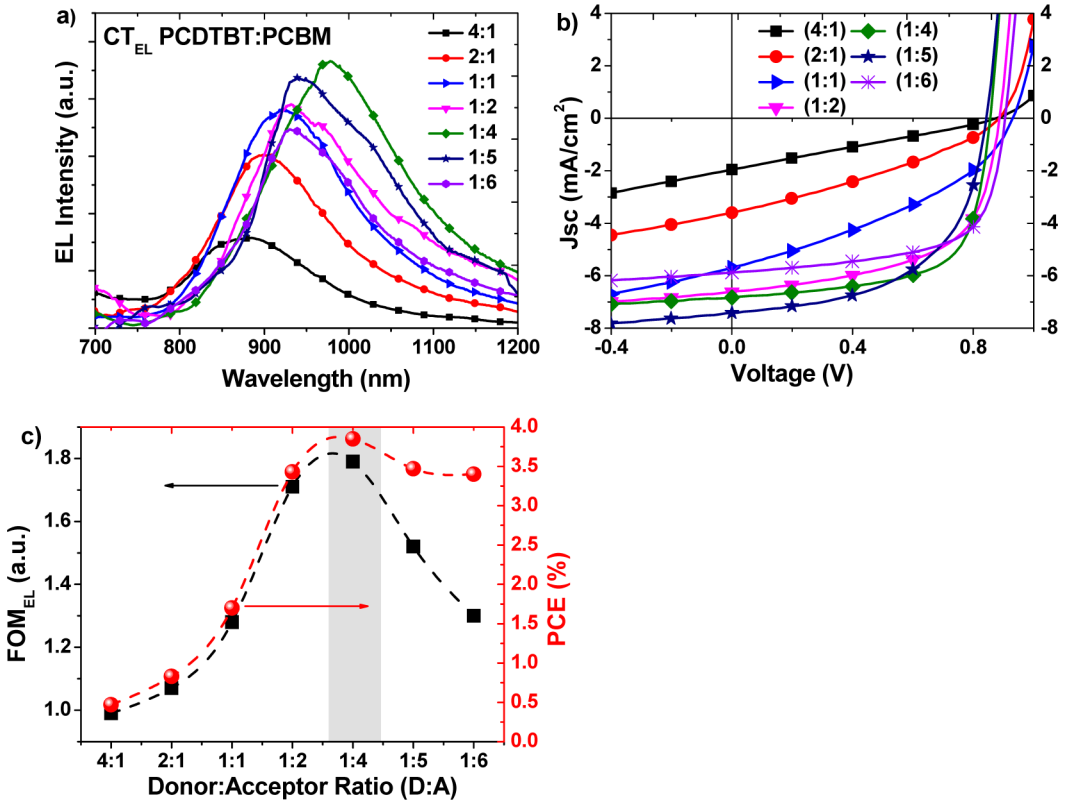

Figure 3. (a) EL spectra of PCDTBT/$PC_{60}BM$ heterojunctions with different stoichiometries. (b) Current–voltage curves of PCDTBT/$PC_{60}BM$ devices using different polymer/fullerene ratios under the illumination of a light source with standard AM 1.5 spectrum with an intensity of 100 mW/cm^2. (c) The FOM_{EL} and PCE trends as a function of PCDTBT/$PC_{60}BM$ ratio. The ratios refer to D/A (w/w). EL measurements and *J*–*V* characteristics were measured for the same device.

benzothia diazole-4,7-diyl-2,5-thiophenediyl] (**PCDTBT**) and a commercial highly efficienct polymer poly[[4,8-bis[(2-ethylhexyl)oxy]benzo[1,2-b:4,5-b′] dithiophene-2,6-diyl][3-fluoro-2-[(2-ethylhexyl)carbonyl]thieno[3,4-*b*]thiophene-diyl]] (**PTB7**) (see Scheme S1 in Supporting Information (SI) for the structures) are used in our studies with different loading ratios of [6,6]-phenyl-C61-butyric acid methyl ester (PCBM or $PC_{60}BM$) to accentuate the validity of this novel, FOM-based method in predicting optimized preparation conditions for solar cells. Furthermore, the approach is undergirded with the construction and verification of an optimization map for active layer deposition using different solvent systems, additives, and additive ratios, without the need for device construction.

RESULTS AND DISCUSSION

In Figure 1a, photoluminescence (PL) and electroluminescence (EL) of pristine PCDTBT (7 mg/mL) films are shown, and the relative PL quenching of the PCDTBT/$PC_{60}BM$ blend is depicted as an inset. The pristine polymer film exhibits a broad PL emission with a maximum at around 725 nm and an EL peak around 730 nm. Addition of $PC_{60}BM$ to pristine polymer quenched 99% of the pristine polymer emission (Figure S2, SI).

dx.doi.org/10.1021/ja503134j | J. Am. Chem. Soc. 2014, 136, 10949–10955

Table 1. Values for the Wavelengths of Maximum PL and EL for the PCDTBT/$PC_{60}BM$ Blends Corresponding to Charge Transfer Emissions (λ_{CT} max), Figures of Merit (FOM_{PL} and FOM_{EL}), and PCEs of the Blends

ratio (D/A)	λ_{CTPL} max (nm)[a]	FOM_{PL} (I_{CT}/I_{S1-S0})[b]	λ_{CTEL} max (nm)[c]	FOM_{EL} (I_{CT}/I_{S1-S0})[b]	PCE (%)[d]
4:1	886	1.05	875	0.99	0.47
2:1	914	1.08	897	1.07	0.83
1:1	917	1.26	920	1.28	1.70
1:2	925	1.79	932	1.71	3.43
1:4	940	1.87	978	1.79	3.85
1:5	896	1.57	940	1.52	3.47
1:6	881	1.49	927	1.30	3.41

[a]Determined from PL spectra. [b]Calculated from I_{CT}/I_{S1-S0}. [c]Determined from EL spectra. [d]Derived from $J-V$ curves of the devices.

Table 2. Summary of the CT_{PL} of Polymer/PCBM Blends That Correspond to Charge Transfer Emissions (I_{CT} max), Figures of Merit (FOM_{PL}) and Performances of the Blends

polymer	ratio (D/A)	λ_{CTPL}[a] (nm)	FOM_{PL}[b]	PCE (%)	polymer	ratio (D/A)	λ_{CTPL}[a] (nm)	FOM_{PL}[b]	PCE (%)
P3HT	4:1		0.12	1.7	PTB7	2:1	1030	0.50	2.1
	2:1	910	0.18	2.4		1:1	970	0.98	4.2
	1.5:1	890	0.25	2.66		1:1.5	952	1.53	5.78
	1:1	885	0.16	2.01		1:2	933	1.35	5.22
	1:2	890	0.10	1.2					
PCDT QxTh-C_8	4:1	830	0.85	0.5	KP115	4:1	986	0.1	0.05
	2:1	900	1.35	0.9		2:1	965	0.15	0.1
	1:1	920	1.66	1.5		1:1	914	0.33	1.05
	1:2	930	2.47	2.8		1:2	920	0.39	2.60
	1:3	910	2.2	2.65		1:3	910	0.50	2.81
	1:4	900	1.96	2.5		1:4	905	0.45	2.67

[a]Determined from PL spectra. [b]Calculated from I_{CT}/I_{S1-S0}.

Figure 1b illustrates the relative PL emissions of PCDTBT/$PC_{60}BM$ thin films, characterized by different weight ratios of $PC_{60}BM$. Upon addition of $PC_{60}BM$, the overall PL is quenched due to the exciton dissociation by the fullerene and a red-shifted, broad emission band peaks at its maximum at ~900 nm and shifts up to 940 nm. This shift is attributed to the charge transfer (CT) emission.[31,32] In literature, it is reported that the polymer emission is totally quenched upon addition of fullerenes to polymers; nevertheless, in most of the cases, residual emission from the singlet will still contribute to the blends emission spectrum.[33] In Figure 1b, this phenomenon can be seen at around 730 nm, where pristine PCDTBT emission occurs because the overall spectrum constitutes both polymer and the charge transfer emission (CTE). Figure 1c shows the residual PCDTBT singlet emission contributions shown in Figure 1b. The total spectrum from Figure 1b is deconvoluted for singlet and CTE in order to have a precise determination of the CTE from PL (Figure 1d).

In what follows, we show that FOM as defined in eq 1 can be used to predict optimized device preparation conditions. We calculate the FOM figures for the composites presented in Figure 1 by dividing the maximum intensities of I_{CT} and I_{SI-S0} obtained from Figure 1d,c, respectively. The comparison between FOM, short-circuit current (J_{SC}) and overall power conversion efficiency (PCE) are summarized in Figure 2 for different PCDTBT/$PC_{60}BM$ ratios.

In Figure 2a, the trend between FOM, J_{SC}, and PCE is shown as a function of D/A ratio. As the $PC_{60}BM$ loading is increased from 20% (4:1) to 80% (1:4), the FOM as well as the short circuit currents and PCE values increase. For very high fullerene loadings >80%, FOM decreased, although the J_{SC} of the PCDTBT/$PC_{60}BM$ devices further increases for the 1:5 ratio. However, the fill factor of the devices decreases (Figure S3, SI). We postulate that a change in morphology at the D/A interface affects the FOM for fullerene loadings higher than 80% affecting mainly FF but also the overall PCE of the cell.[33] Figure 2b summarizes the relation between the FOM and the PCE of the devices. Most noteworthy, we find an excellent correlation between FOM and PCE, and indeed, the composites with highest FOM result in devices with highest photocurrent generation yield and PCE. Although FOM does not consider the electrical contacts and transport in the cell, it is strongly correlated to the J_{SC} and morphology of the blend which affects the CT formation.

We further confirmed this method by utilizing electroluminescence spectroscopy, where CT emission is observed due to recombination of injected charge carriers.[31] Unlike photoluminescence, electroluminescence measurements involve carrier transport, which affects the FF.[34] Figure 3a summarizes the EL_{CT} measurement as a function of fullerene loading, whereas Figure 3b shows the $J-V$ data for the various composites. As expected, higher $PC_{60}BM$ ratios result in higher EL signals (at constant current) correlates with J_{SC}. We calculated the FOM for the electroluminescence spectra. Once more, an excellent trend is observed between the figure of merit and the device performances (Figure 3c).[35] One can argue that FOM_{EL} is most suitable to correlate with the PCE value because EL measurements include charge transport. It is however clear from both PL and EL data sets that both FOM_{EL} and FOM_{PL} can be used as guides to optimize device fabrication parameters. Moreover, we want to stress that the FOM_{EL} evaluation requires the production of fully functional devices, whereas the FOM_{PL} evaluation was simply done using thin films of active layers deposited on glass/PEDOT. Using FOM_{PL} as optimization guideline is thus very advantageous, given the striking correlation between PCE and FOM_{PL}.

dx.doi.org/10.1021/ja503134j | J. Am. Chem. Soc. 2014, 136, 10949−10955

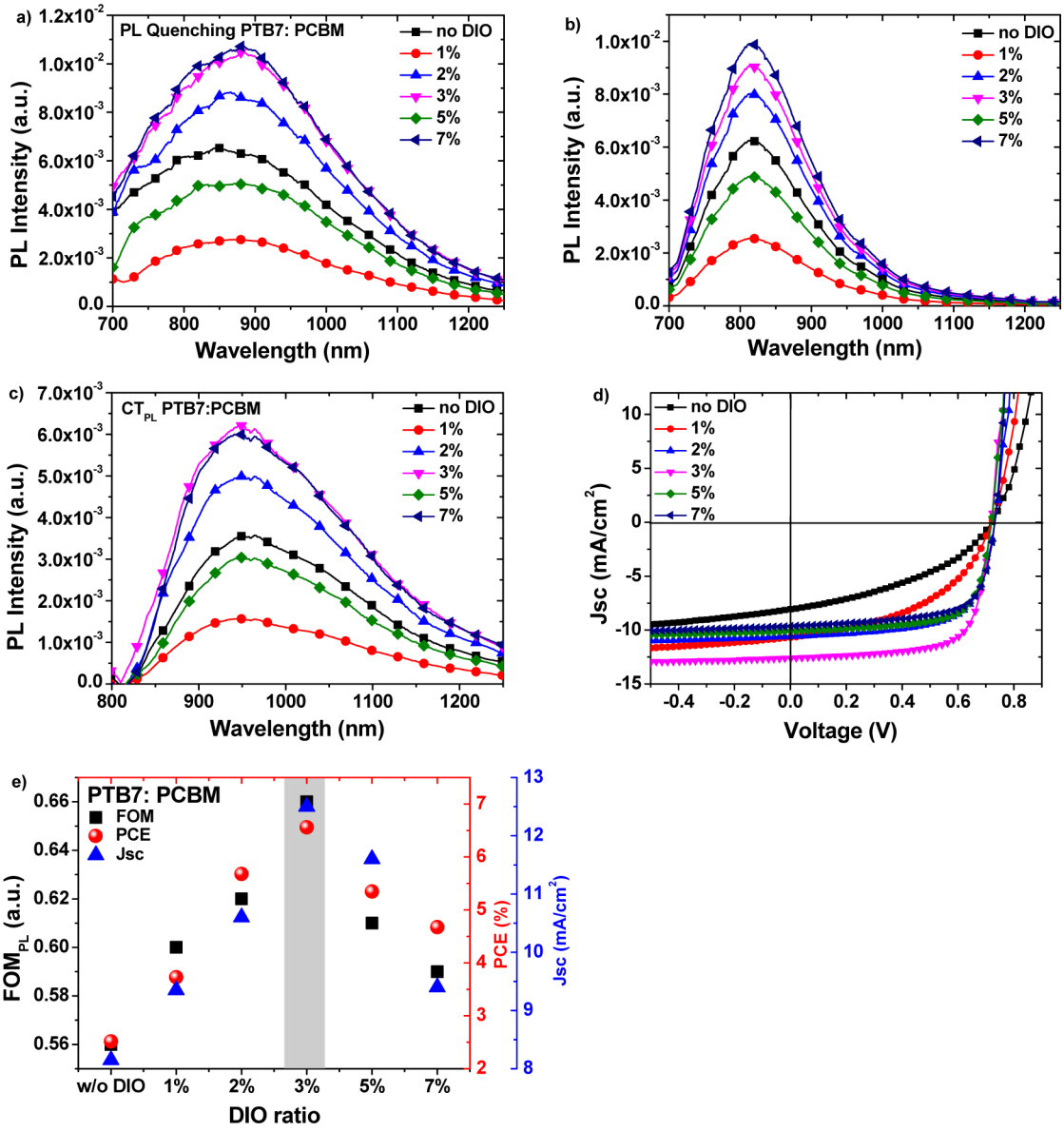

Figure 4. (a) PL quenching of PTB7/$PC_{60}BM$ blends without DIO and with various DIO ratios, (b) singlet contributions in the blends, (c) charge transfer emissions after subtraction of residual singlet emission, (d) device performances of PTB7/$PC_{60}BM$ cells varying additive ratio, and (e) correlation between FOM (square), PCE (circle) and J_{SC} (triangle) vs additive ratio for PTB7/PCBM blends with different DIO ratios.

The most significant results for the investigated PCDTBT/$PC_{60}BM$ blends are summarized in Table 1. According to Table 1, CT emissions from both PL and EL are most red-shifted for the best PCDTBT/$PC_{60}BM$ ratio (1:4) where the singlet emission from the polymer is the smallest, and the overall emission is dominated by the CT state. Furthermore, the trend of FOM values precisely follows the PCEs of the respective devices.

The simplicity of PL motivated us to apply this elegant strategy to the very well-known commercial polymer P3HT. P3HT is mixed with $PC_{60}BM$ at different ratios and devices are constructed to find the optimized D/A ratio and $J-V$ curves were measured in order to compare J_{SC} and PCE with the FOM calculated from photoluminescence measurements (Figure S4, SI). The results are summarized in Table 2. The highest FOM corresponds to the best P3HT/$PC_{60}BM$ ratio (1.5:1). These fascinating results encouraged us to broaden the applicability of this method to other optimized system KP115/$PC_{60}BM$ and PTB7/$PC_{60}BM$ (3% DIO). The striking correlations for the best D/A ratios were once more observed using FOM method (Figure S5, SI). The best PCE 2.8% for KP115/$PC_{60}BM$ resulted in the highest FOM of 0.5. For PTB7 system used with 3% DIO, similar outcomes were observed for different $PC_{60}BM$ loadings (Table 2). However, one can argue that this method may prove already optimized systems, because one could estimate the performance potential from previously constructed devices. That is why the same approach is applied to an new system PCDTQxTh-C8/$PC_{60}BM$ which was synthesized by Leclerc group (Figure S6, SI). First, only active layer thin films were coated simply on glass/PEDOT. Subsequently, PL studies were carried out and the FOM was determined. The 1:2 PCDTQxTh-C8/$PC_{60}BM$ ratio was found to have the highest FOM value which was afterward confirmed by device fabrication (Table 2). These findings instigated further optimization studies using photoluminescence as an elegant method in order to explore further optimization strategies.

dx.doi.org/10.1021/ja503134j | J. Am. Chem. Soc. 2014, 136, 10949−10955

In addition to varying the D/A composition to optimize a solar cell system, solvent or solvent processing additives can be an alternative for further optimization.[11,36,37] For many polymer systems, 1,8-diiodooctane (DIO) showed the highest PCE enhancement to date.[38−41] We used the high PCE donor material PTB7 to extend our study to additive ratio variation for the PTB7/$PC_{60}BM$ (1:1.5) system and investigate the influence of the DIO/solvent ratio on the FOM, J_{SC}, and PCE. Figure 4 demonstrates how FOM is correlated to the device parameters. The addition of a small amount of DIO to PTB7/$PC_{60}BM$ system quenches the emission; however, higher loadings of DIO to the blend show higher PL intensity due to the formation larger domains in the bulk. The $J-V$ characteristics point out that 3% DIO addition results in the highest PCE in PTB7/$PC_{60}BM$ solar cells. The best cell has the highest FOM and showed a 6.7% PCE when $PC_{60}BM$ is used as an acceptor in the inverted structure.

The idea that a PL FOM can be used in order to quickly and reliably scan the optimized processing conditions for composites is proven for various donor/$PC_{60}BM$ systems. Nevertheless, we were still not satisfied by simply varying the D/A ratio or the additive ratio. We also investigated combinatorial methods by altering two different parameters, the type of solvent and the additive, to further optimize the PTB7/$PC_{60}BM$ system. A 3D FOM map is obtained for PTB7/$PC_{60}BM$ blends. The previously optimized 1:1.5 ratio is used for the polymer/$PC_{60}BM$ ratio, and a 3% additive ratio was kept constant.

Figure 5 demonstrates a bar map which can be used for determination of the optimized combined processing conditions for PTB7/$PC_{60}BM$ solar cells. The FOM map predicted that 3% DIO for 1:1.5 PTB7/$PC_{60}BM$ system in cholorobenzene (CB) are the best processing conditions among the ones investigated. The solar cells prepared using these preparation conditions yielded a PCE of (~7%). Our results based on combinatorial mapping methods can be used to control and optimize the solar cells using PL without arduous work. In this part of discussion, it would not be discursive to mention that we are aware there might be limitations to determine the figure of merit. It is well-known in the literature that despite the significance of CT states for organic photovoltaics, their direct spectral identification has only been achieved in a limited amount of materials.[19,22,42] Weak CT state absorption and emission or preferred nonradiative processes rather than radiative recombination to ground state may restrain the detection of CT states through optical methods.

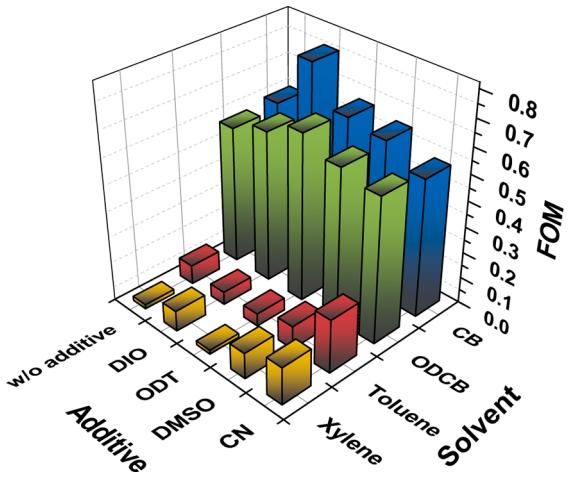

Figure 5. Figure of merit values (z-axis) versus different solvent and additive systems for PTB7/$PC_{60}BM$ (1:1.5). The highest figure of merit corresponds to the best solar cell condition.

CONCLUSION

In summary, we have shown a systematical investigation of a contactless method to anticipate the optimized device parameters for several commonly used polymers by solely evaluating the photoluminescence properties. A representative figure of merit is calculated by taking the ratio between charge transfer emissions (I_{CT}) and residual polymer singlet emissions (I_{S1-S0}). The ratio I_{CT}/ I_{S1-S0} from photoluminescence as well as electroluminescence is correlated to the PCE and J_{SC} of the corresponding devices to anticipate the optimized parameters without device fabrication. Combinatorial mapping for PTB7/$PC_{60}BM$ system revealed the applicability of this method as a fast and reliable test for the optimization of bulk heterojunction composites. The contactless method is easily automated and integrable, and as such, we believe that the FOM concept will deliver valuable information for the material development and process optimization communities. Further optimizations and combinatorial methods can be carried out to broaden the employment of this method.

ASSOCIATED CONTENT

Supporting Information

Description of the material included, including chemical structures, energy level diagram, and photoluminescence data as referenced in the text. This material is available free of charge via the Internet at http://pubs.acs.org.

AUTHOR INFORMATION

Corresponding Authors

*E-mail: christoph.brabec@fau.de
*E-mail: derya.baran@fau.de

Present Address

[‖]Corporation Scientifique Claisse, 350 rue Franquet, Suite 45, Quebec, Quebec, Canada G1P 4P3.

Notes

The authors declare no competing financial interest.

ACKNOWLEDGMENTS

The authors gratefully acknowledge the Cluster of Excellence "Engineering of Advanced Materials" at the University of Erlangen-Nuremberg, which is funded by the German Research Foundation (DFG) within the framework of "Excellence Initiative", Bavarian Research Foundation (BSF), and the project Synthetic Carbon Allotropes (SFB953). This work was cofunded by the European Regional Development Fund and the Republic of Cyprus through the Research Promotion Foundation (Strategic Infrastructure Project NEA ΥΠΟ-ΔΟΜΗ/ΣΤΡΑΤΗ/·0308/06). N. Li acknowledges the financial support of the European Commission as part of the Framework 7 ICT 2009 collaborative project ROTROT ("roll to roll production of organic tandem cells", Grant no. 288565) project.

REFERENCES

(1) Green, M. A.; Emery, K.; Hishikawa, Y.; Warta, W.; Dunlop, E. D. *Prog. Photovoltaics* **2012**, *20*, 12.

(2) Ameri, T.; Dennler, G.; Waldauf, C.; Denk, P.; Forberich, K.; Scharber, M. C.; Brabec, C. J.; Hingerl, K. *J. Appl. Phys.* **2008**, *103*, 084506.
(3) Yang, T.; Wang, M.; Duan, C.; Hu, X.; Huang, L.; Peng, J.; Huang, F.; Gong, X. *Energy Environ. Sci.* **2012**, *5*, 8208.
(4) Saeki, A.; Yoshikawa, S.; Tsuji, M.; Koizumi, Y.; Ide, M.; Vijayakumar, C.; Seki, S. *J. Am. Chem. Soc.* **2012**, *134*, 19035.
(5) Teichler, A.; Eckardt, R.; Hoeppener, S.; Friebe, C.; Perelaer, J.; Senes, A.; Morana, M.; Brabec, C. J.; Schubert, U. S. *Adv. Energy Mater.* **2011**, *1*, 105.
(6) Clarke, T. M.; Durrant, J. R. *Chem. Rev.* **2010**, *110*, 6736.
(7) Grozema, F. C.; Siebbeles, L. D. A. *J. Phys. Chem. Lett.* **2011**, *2*, 2951.
(8) Guo, X.; Zhang, M.; Tan, J.; Zhang, S.; Huo, L.; Hu, W.; Li, Y.; Hou, J. *Adv. Mater.* **2012**, *24*, 6536.
(9) Yao, Y.; Hou, J.; Xu, Z.; Li, G.; Yang, Y. *Adv. Funct. Mater.* **2008**, *18*, 1783.
(10) Moulé, A. J.; Meerholz, K. *Adv. Mater.* **2008**, *20*, 240.
(11) Scharber, M. C.; Lungenschmied, C.; Egelhaaf, H.-J.; Matt, G.; Bednorz, M.; Fromherz, T.; Gao, J.; Jarzab, D.; Loi, M. A. *Energy Environ. Sci.* **2011**, *4*, 5077.
(12) Wang, E.; Ma, Z.; Zhang, Z.; Vandewal, K.; Henriksson, P.; Inganäs, O.; Zhang, F.; Andersson, M. R. *J. Am. Chem. Soc.* **2011**, *133*, 14244.
(13) Tan, Z. a.; Zhang, W.; Zhang, Z.; Qian, D.; Huang, Y.; Hou, J.; Li, Y. *Adv. Mater.* **2012**, *24*, 1476.
(14) Guerrero, A.; Montcada, N. F.; Ajuria, J.; Etxebarria, I.; Pacios, R.; Garcia-Belmonte, G.; Palomares, E. *J. Mater. Chem. A* **2013**, *1*, 12345.
(15) Ameri, T.; Heumuller, T.; Min, J.; Li, N.; Matt, G.; Scherf, U.; Brabec, C. J. *Energy Environ. Sci.* **2013**, *6*, 1796.
(16) Li, K.; Khlyabich, P. P.; Li, L.; Burkhart, B.; Thompson, B. C.; Campbell, J. C. *J. Phys. Chem. C* **2013**, *117*, 6940.
(17) Boix, P. P.; Guerrero, A.; Marchesi, L. F.; Garcia-Belmonte, G.; Bisquert, J. *Adv. Energy Mater.* **2011**, *1*, 1073.
(18) Liedtke, M.; Sperlich, A.; Kraus, H.; Baumann, A.; Deibel, C.; Wirix, M. J. M.; Loos, J.; Cardona, C. M.; Dyakonov, V. *J. Am. Chem. Soc.* **2011**, *133*, 9088.
(19) Tvingstedt, K.; Vandewal, K.; Gadisa, A.; Zhang, F.; Manca, J.; Inganäs, O. *J. Am. Chem. Soc.* **2009**, *131*, 11819.
(20) Schlenker, C. W.; Chen, K.-S.; Yip, H.-L.; Li, C.-Z.; Bradshaw, L. R.; Ochsenbein, S. T.; Ding, F.; Li, X. S.; Gamelin, D. R.; Jen, A. K. Y.; Ginger, D. S. *J. Am. Chem. Soc.* **2012**, *134*, 19661.
(21) Deibel, C.; Strobel, T.; Dyakonov, V. *Adv. Mater.* **2010**, *22*, 4097.
(22) Hallermann, M.; Kriegel, I.; Da Como, E.; Berger, J. M.; von Hauff, E.; Feldmann, J. *Adv. Funct. Mater.* **2009**, *19*, 3662.
(23) Loi, M. A.; Toffanin, S.; Muccini, M.; Forster, M.; Scherf, U.; Scharber, M. *Adv. Funct. Mater.* **2007**, *17*, 2111.
(24) Keivanidis, P. E.; Kamm, V.; Dyer-Smith, C.; Zhang, W.; Laquai, F.; McCulloch, I.; Bradley, D. D. C.; Nelson, J. *Adv. Mater.* **2010**, *22*, 5183.
(25) Luo, Y.; Aziz, H. *Adv. Funct. Mater.* **2010**, *20*, 1285.
(26) Dimitrov, S. D.; Durrant, J. R. *Chem. Mater.* **2013**, *26*, 616.
(27) Servaites, J. D.; Ratner, M. A.; Marks, T. J. *Appl. Phys. Lett.* **2009**, *95*, 163302.
(28) Vandewal, K.; Tvingstedt, K.; Gadisa, A.; Inganas, O.; Manca, J. V. *Nat. Mater.* **2009**, *8*, 904.
(29) Vandewal, K.; Albrecht, S.; Hoke, E. T.; Graham, K. R.; Widmer, J.; Douglas, J. D.; Schubert, M.; Mateker, W. R.; Bloking, J. T.; Burkhard, G. F.; Sellinger, A.; Fréchet, J. M. J.; Amassian, A.; Riede, M. K.; McGehee, M. D.; Neher, D.; Salleo, A. *Nat. Mater.* **2014**, *13*, 63.
(30) Scharber, M. C.; Sariciftci, N. S. *Prog. Polym. Sci.* **2013**, *38*, 1929.
(31) Faist, M. A.; Kirchartz, T.; Gong, W.; Ashraf, R. S.; McCulloch, I.; de Mello, J. C.; Ekins-Daukes, N. J.; Bradley, D. D. C.; Nelson, J. *J. Am. Chem. Soc.* **2011**, *134*, 685.
(32) Piersimoni, F.; Cheyns, D.; Vandewal, K.; Manca, J. V.; Rand, B. P. *J. Phys. Chem. Lett.* **2012**, *3*, 2064.
(33) Veldman, D.; Aipek, O. z.; Meskers, S. C. J.; Sweelssen, J. r.; Koetse, M. M.; Veenstra, S. C.; Kroon, J. M.; Bavel, S. S. v.; Loos, J.; Janssen, R. A. J. *J. Am. Chem. Soc.* **2008**, *130*, 7721.
(34) Ma, Z.; Tang, Z.; Wang, E.; Andersson, M. R.; Inganäs, O.; Zhang, F. *J. Phys. Chem. C* **2012**, *116*, 24462.
(35) Vandewal, K.; Tvingstedt, K.; Gadisa, A.; Inganas, O.; Manca, J. V. *Nat. Mater.* **2009**, *8*, 904.
(36) Machui, F.; Rathgeber, S.; Li, N.; Ameri, T.; Brabec, C. J. *J. Mater. Chem.* **2012**, *22*, 15570.
(37) Lou, S. J.; Szarko, J. M.; Xu, T.; Yu, L.; Marks, T. J.; Chen, L. X. *J. Am. Chem. Soc.* **2011**, *133*, 20661.
(38) Cabanetos, C.; El Labban, A.; Bartelt, J. A.; Douglas, J. D.; Mateker, W. R.; Fréchet, J. M. J.; McGehee, M. D.; Beaujuge, P. M. *J. Am. Chem. Soc.* **2013**, *135*, 4656.
(39) Kim, D. H.; Ayzner, A. L.; Appleton, A. L.; Schmidt, K.; Mei, J.; Toney, M. F.; Bao, Z. *Chem. Mater.* **2012**, *25*, 431.
(40) Lee, J. K.; Ma, W. L.; Brabec, C. J.; Yuen, J.; Moon, J. S.; Kim, J. Y.; Lee, K.; Bazan, G. C.; Heeger, A. J. *J. Am. Chem. Soc.* **2008**, *130*, 3619.
(41) Li, W.; Hendriks, K. H.; Furlan, A.; Roelofs, W. S. C.; Wienk, M. M.; Janssen, R. A. J. *J. Am. Chem. Soc.* **2013**, *135*, 18942.
(42) Manca, M.; Piliego, C.; Wang, E.; Andersson, M. R.; Mura, A.; Loi, M. A. *J. Mater. Chem. A* **2013**, *1*, 7321.